MRS Advances © 2016 Materials Research Society
DOI: 10.1557/adv.2016.236

Substrates with Programmable Heater Arrays for In-Situ Observation of Microstructural Evolution of Polycrystalline Films: Towards Real Time Control of Grain Growth

Prabhu Balasubramanian[1], Chengjian Zheng[2], Yixuan Tan[2], Genevieve Kane[1], Antoinette Maniatty[2], John Wen[3,4], and Robert Hull[1]

[1]Department of Materials Science and Engineering, [2]Department of Mechanical, Aerospace and Nuclear Engineering, [3]Department of Industrial and Systems Engineering, [4]Department of Electrical and Computer Systems Engineering, Rensselaer Polytechnic Institute, 110 8th Street, Troy, NY 12180

ABSTRACT

An integrated experimental – simulation – control theory approach designed to enable adaptive control of microstructural evolution in polycrystalline metals is described. A micro-heater array, containing ten addressable channels, is used to create desired temperature profiles across thin polycrystalline films *in situ* to a scanning electron microscope (SEM). The goal is that on heating with controlled temperature profiles, the evolution of grain growth within the film can be continuously monitored and compared to Monte Carlo simulations of trajectories towards a desired microstructure. Feed-forward and feedback control strategies are then used to guide the microstructure along the desired trajectory.

INTRODUCTION

The macroscale engineering properties of metals are directly linked to microstructural characteristics, which, in turn, are generated during thermo-mechanical processing. Thus, controlling the processing conditions to create a desired microstructure and resulting macroscale properties is a major priority for materials manufacturers [e.g. 1,2] and for the Materials Genome Initiative [3]. This work focuses on developing the methodology and algorithms necessary to actively control materials processing to achieve a target microstructure.

Our approach employs *in situ* materials processing and sensing within a SEM to directly monitor grain structure evolution during annealing. We have developed an independently controllable ten-zone resistive micro-heater array that can be operated within the SEM. Secondary electron imaging is used to measure the evolution of grain size distributions in polycrystalline Cu films, while electron backscattered diffraction (EBSD) and a novel temperature sensitive technique derived from EBSD [4] will be employed to monitor crystallography and local temperature in real time. The observed grain growth trajectories are compared to Monte Carlo (MC) grain growth models. The information from modeling and real time observation (and specifically triggered by deviations between the two), will then be combined into feed-forward and feedback control strategies for real-time control of microstructure evolution. This approach is summarized in Figure 1.

DESIGN AND FABRICATION OF THE HEATER ARRAY

The micro-heater arrays were fabricated using methods similar to those described by Darhuber et al. [5]. A set of ten individually, electrically addressable Ti lines are fabricated within a SiO_2 matrix, upon a Si substrate (Figure 2). A 1-4 μm polycrystalline Cu film is then deposited over the top SiO_2 film. Finite element analysis is used to design the structure such that the overall array can be heated to 200-300°C using an SEM heater stage, and resistive heating of the Ti heater lines can provide an additional range of 0-100°C of heating. The current density in

the Ti lines should be <10^6 A/cm^2 to avoid rapid failure due to electromigration. The active heated area of Cu is a fraction of a mm^2, consistent with the available field of view during SEM imaging. This translates into a pitch of 100 µm between adjacent heater lines. As an example, finite element modeling for Ti wires of 70 µm width and 400 nm thickness and current (density) of 240 mA (8.5 x 10^5 Acm^{-2}) through each line, show a maximum temperature within the heated region of 380°C when the underlying substrate is held at 200°C.

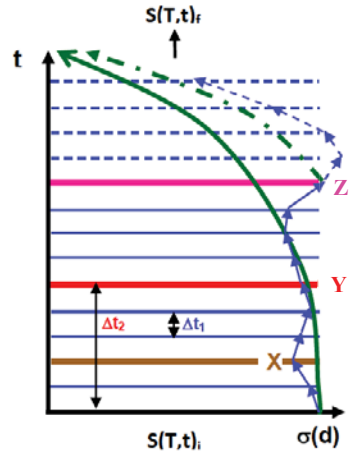

Figure 1. Scheme for mapping of real time observations of simulated trajectories. A micro-structural figure of merit (e.g., variation in mean grain size, σ(d)) is assessed at regular intervals through analysis of SEM images (indicated horizontal lines with time increment Δt_1). Periodically, a more complete crystallographic analysis is performed using EBSD (e.g at point Y) with time increment Δt_2. The observed experimental trajectory for σ (d), indicated by short vectors, is compared to the simulated trajectory, curved solid line. Trajectory differences between experiment and simulation, e.g., at point X, are corrected by adjusting the temperature field based on the gradient of σ (d) with respect to the heater input. Major differences between experiment and simulation, e.g., at point Z require a full Monte Carlo-based re-optimization of the microstructural trajectory from the new starting conditions (dot-dashed curve). Experimental implementation of the new trajectory is then implemented through feed-forward control of the array of heater inputs.

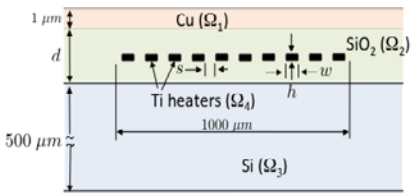

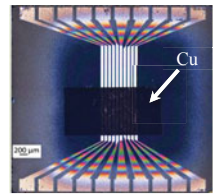

Figure 2: Left- Schematic cross-section of the heater array design. Right – Optical image of the fabricated heater array

An optical image of the fabricated heating array, with an electron-beam deposited copper film over the central part is shown in Figure 2 (the Ti lines appear visible through the Cu because of surface topography). In brief, these arrays were fabricated as follows upon a 2" Si(100) wafer. Following O_2 plasma cleaning of the surface, a 2.5 µm SiO_2 layer was deposited at 300° C by plasma enhanced chemical vapor deposition. Next, the array of heating lines was fabricated by electron beam evaporation of a 400 nm thick Ti film, and patterned with conventional contact optical lithography to create a PMMA resist mask for a buffered oxide etch. A second set of lithographic processes then created the Al contact lines to each of the Ti heater lines, and an additional 1-3 µm SiO_2 layer was deposited on top the heater line arrays. (All thicknesses quoted here are nominal). Multiple arrays were fabricated over the 2" wafer and then cut into c. 1 cm^2 square chips, mounted onto a chip carrier, and the Al contact pads for each heater line element gold wire bonded to contacts on the carrier.

MODELING AND SIMULATION

There is an extensive literature on modeling of grain growth in metals [e.g. 6-8]. In our MC simulations, we use the Potts [e.g. 8] construction. The domain is discretized into a set of N lattice points with lattice spacing λ. Next a lattice point is randomly selected and its orientation changed to one of its neighbors. If the system energy is reduced or unchanged, then the orientation change is accepted, otherwise, the probability of the change being accepted exponentially decreases with the increase in system energy. One MC step is defined as N reorientation attempts. Both classical grain growth theory and the MC predictions follow a parabolic grain growth relationship such that the mean grain size D evolves in time t according to

$$D^2 - D_0^2 = Kt\, e^{-Q/kT} = K_{MC}\lambda^2 S_{MC} \qquad - (1)$$

Where D_0, K, Q, K_{MC}, and S_{MC} represent the initial grain size, physical growth constant, activation energy, MC growth constant, and number of MC steps, respectively [9]. The activation energy for grain growth in Cu films has been determined to be Q = 1.55 eV [10]. By equating the mean grain size in the experiment and simulation and fitting the experimental and simulation results to the above equation, we find $K = 9.4 \times 10^8$ μm²/s and $K_{MC} = 1.43$.

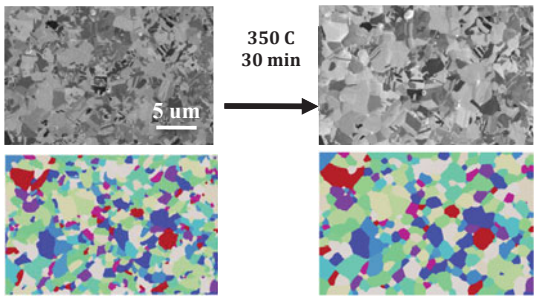

Figure 3: Experimental microstructures in a 2.6 μm Cu film (top) before and after a 350°C, 30 minute anneal in the SEM. Isotropic MC simulations (bottom) are initialized to the initial microstructure and then annealed until the average simulated grain size matches that in the post-annealed (the differently colored grains in the simulations are for visualization only).

Initial matching of isotropic simulations to experimental data for uniform heating are performed to refine our comparison methods, as shown in Figure 3. The MC simulations are initialized to the starting grain structure and then run until the mean grain sizes match very close to those of the experimentally annealed microstructure. The points of comparison between experiment and simulation are then the standard deviation and kurtosis of the grain size distributions. (The grain boundaries are currently manually defined using a set of rules we have developed to delineate grain edges and differentiate, for example, grain boundaries from twin boundaries within a grain. As a test of observer bias, two separate trials of grain boundary delineation by two separate observers using this set of rules, over fields of view of several hundred μm² containing several hundred grains, yielded mean, standard deviation and kurtosis of grain sizes that agreed within a few percent between the two trials).

It is found that both the standard deviation and the kurtosis of the experimental distributions for this particular comparison set are slightly higher than the simulated distributions. We note that such observations are sensitive to the initial grain distributions – a set of four comparisons between experimental and simulated anneals showed standard deviations that differed by a few percent and kurtoses that differed by a few tens of percent. Work is ongoing to more systematically compare experimental vs. simulated distributions.

	Initial			Annealed		
	Mean $(\mu m)^2$	Standard Deviation $(\mu m)^2$	Kurtosis	Mean $(\mu m)^2$	Standard Deviation $(\mu m)^2$	Kurtosis
Experiment	0.70	0.84	13.8	1.19	1.33	8.99
Simulation	0.70	0.84	13.8	1.20	1.24	8.22

Table 1: Comparison of simulated and experimental grain area (D^2) before and after annealing (350 ^oC, 30 mins). The initial distributions are equivalent, as the MC simulation is initialized to the pre-anneal experimental distribution. The MC structures are annealed until the mean grain area is very close to that of the experimental structures; and the resulting standard deviations and kurtoses compared.

HEATER ARRAY CONTROL

The overarching goal of this work is to use feed-forward and feedback control algorithms to guide experimental grain growth along the thermal trajectories (estimated by simulation) that result in desired distributions of grain microstructure and hence mechanical properties. This is enabled by independent control of the individual heater elements in the ten-channel micro-heater array to individually control their temperatures, and hence the resulting temperature profile across the copper film, and thus the distribution of grain sizes across the film. The desired final microstructure might be as uniform a grain size as possible, with a given mean size and low standard deviation and kurtosis, or a linearly graded grain size, or more complex distributions.

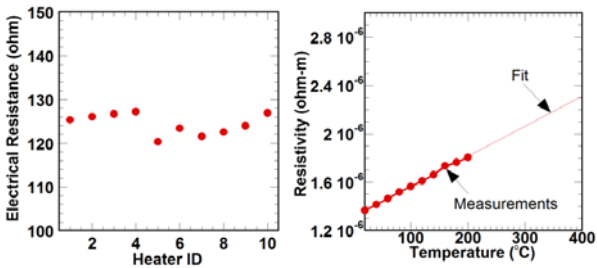

Figure 4: Left – individual heater element resistances across a ten channel heater array (we estimated errors including contact resistances to be c. 2Ω). Right – measured resistivity as a function of temperature for one heater line.

We have integrated the experimental, simulation and control cycle in multiple configurations, preparatory to realizing the full control algorithms in real time in the SEM. For example, control algorithms have been developed to control the individual heater elements within the finite element model of the heater array to virtually create desired temperature profiles across the Cu surface [11,12]. At a greater level of complexity, we have also developed algorithms to couple the temperature distributions from the finite element model to Monte Carlo simulations of grain growth. The simulated grain sizes from each of ten zones associated with the spatial location of the underlying heater elements are then used as the output variables to inform the control algorithm as to what heater inputs will drive the system towards the desired grain distribution. Here, however, we focus on control of the experimental system.

Fig. 4(a) shows the individual resistances of each of the heater elements in a particular array, while Fig. 4(b) shows the dependence of resistivity upon temperature for one of the heater channels determined using an external heating source (the mount of the Keithley probe station in which the I-V measurements were made) for temperatures up to 200°C, with linear extrapolation to higher temperatures. (The resistivity of non-magnetic metals varies close to proportionally to

temperature in this range, e.g. [13]). Note also that these measurements were made on an array prior to deposition of the capping SiO_2 layer and the Cu film). The room temperature resistivity, c. 1.3 x 10^{-6} Ωm, is about a factor three higher than "bulk" values. We attribute these differences primarily to the Ti film microstructure and in particular its relatively small Ti grain size (< 100 nm) in our films (strong dependences in resistivity have been observed as a function of grain size and film thickness, for example, in [14], albeit with comparable magnitudes at somewhat thinner films and smaller grain sizes than those in this work). The measured resistivity of the Ti heater elements may thus be used as an internal calibration of temperature as we run currents through them. In general we note that measured Ti line resistances and resistivities do vary somewhat within a given array, depending primarily on the variation in Ti heater line widths, which are typically within ± 5% (corresponding to ΔT c. ± 30° C depending on temperature) within a given array. Thus the most careful control calibrations require separately measuring the individual heater element resistances, and temperature dependent resistivities, for each completed chip. We also note that temperatures between the heater lines themselves and the surface of the chip differ by less than 4° C from FEM calculations.

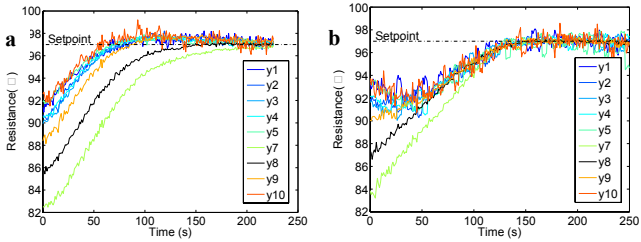

Figure 5. Control of heater line resistances ex-situ to the SEM. (a) Decentralized control algorithm (b) With consensus augmentation.

Figure 5 shows proof of principle of heater line control ex-situ to the SEM, driving individual resistances to a 100 Ω set point, when the individual resistances in this particular chip vary from about 82 Ω to 92 Ω. The major control constraints applied to the algorithms employed for this particular goal state were (i) to reach the desired setpoints and (ii) to reach those setpoints while minimizing the transient temperature gradient across the sample, to minimize possible thermal stresses. We stress that for the heater array controlled in Figure 5, the heater elements are very close to each other (90 μm line widths with 10 μm spacings), so the temperature fields from adjacent heaters overlap very strongly and thus are highly interactive, creating a more complex control challenge. In the left figure, a fully decentralized control algorithm is applied (i.e. control of each line is based on the deviation of the line resistance from its setpoint). The resistances – and hence the temperatures – converge relatively rapidly (a few minutes) towards their set points, but the spread of resistances of the lines remains relatively large until convergence, creating transient temperature distributions and possible thermal stresses. In the right figure, consensus augmentation methods are used where the control increments on each heater line current has a controlled dependence on the control increments on neighboring lines (see Refs [11,12] for further details). While the time to final convergence to the setpoint is comparable in the two cases, the convergence of the individual lines' resistance to each other is significantly more rapid for the consensus case.

We are currently integrating this full experimental and control system into an FEI Versa dual scanning electron and ion beam instrument, and have obtained preliminary in-situ results on temperature control and grain growth.

CONCLUSIONS

We are developing the capability for real-time active control of materials microstructure during thermal processing, with the initial focus being polycrystalline grain growth in Cu thin films. To this end, we have designed, modeled and fabricated a ten-zone micro-heater array using Ti resistive heater elements for use during in-situ imaging of grain evolution in an SEM, with the goal of independently controlling the individual heater elements to drive the system towards a desired final microstructure. The trajectories towards the target microstructure are defined by Monte Carlo simulations; initial comparison of these trajectories to real time experimental observations of grain growth show relatively good matches on grain size distributions. We have implemented feedback and feed-forward control algorithms to drive surface temperatures in finite element models of the heater array to desired distributions, and used these surface temperature distributions to drive grain growth in a Monte Carlo model, employing simulated grain sizes as input variable for the control loops, and driving experimental temperatures in the heater array to desired profiles. Full integration of the heater array, sensor measurement methods, simulation, and control algorithms in-situ to the SEM are in progress, with initial results on heater control and grain growth obtained. While we are focusing initially on the specific example of thermally driven grain growth in polycrystalline Cu films, we are also exploring how broadly these real-time adaptive control approaches may be applied in materials processing.

ACKNOWLEDGMENTS

We acknowledge extensive use of fabrication and characterization facilities with the Center for Materials, Devices and Integrated Systems (cMDIS) at RPI, and J. Barthel, B. Colwill, R. Dove, M.D. Frey, D. Rende and K. Way for technical expertise. We acknowledge project members D. Crist, T. Keller and D. Lewis for collaboration with phase field modeling and T. Valdez for grain size algorithms and measurements. This work was supported by NSF-DMREF, award number 1334283.

REFERENCES

[1] Copper Applications Technology Roadmap. Inter Copper Assoc, Ltd. (New York,NY, 2011).
[2] Aluminum Technology Roadmap. The Aluminum Association (Washington, DC, 2003).
[3] https://www.whitehouse.gov/mgi (accessed on 01/04/16).
[4] X. Wu and R. Hull, Nanotechnology **23**: 465707:1-7, 2012.
[5] A.A. Darhuber, S.M. Troian and S. Wagner, J. Appl. Phys. **91**: 5686-92, 2002.
[6] C.V. Thompson, Ann. Rev. Mat. Sci. **20**, 245-68 (2002)
[7] A.D. Rollett, A.P. Brahme and C.G. Roberts, Mat. Sci. For. **588-9**, 33-42, 2007
[8] M. P. Anderson, D. J. Srolovitz, G. S. Grest, and P. S. Sahni, Acta Metall. 32:783–791, 1984.
[9] J. Gao and R. Thompson, Acta materialia, **44**, 4565-70, 1996.
[10] A. Gangulee, J. Appl. Phys. **45**, 3749-56, 1974.
[11] C. Zheng, Y. Tan, J.T. Wen, and A.M. Maniatty, Proc. American Control Conference, Chicago, IL, p. 619-24 (IEEE, Piscataway, NJ, 2015)
[12] Y. Tan, C. Zheng, J.T. Wen, A.M. Maniatty, Inverse Problems in Sci. & Eng, submitted.
[13] S.O. Kasap, Principles of Electronic Materials & Devices, (2nd ed. McGraw-Hill), 2.3, 2002
[14] M.E. Day, M. Delfino, J.A. Fair, and W. Tsai, Thin Solid Films **254**, 285-90 (1995)